Journal of Colloid and Interface Science **212,** 545–552 (1999)
Article ID jcis.1998.6062, available online at http://www.idealibrary.com on IDEAL®

Formation of Ultrathin Films at the Solid–Liquid Interface Studied by *In Situ* Ellipsometry

Helmut Brunner, Thomas Vallant, Ulrich Mayer, and Helmuth Hoffmann[1]

Department of Inorganic Chemistry, Vienna University of Technology, Getreidemark 9, A-1060, Wien, Austria

E-mail: hhoffman@email.tuwien.ac.at

Received October 9, 1998; accepted December 17, 1998

Ellipsometric investigations of self-assembled monolayers (SAMs) of alkylsiloxanes on native silicon substrates and of organothiols on gold substrates were performed under *in situ* conditions with the substrate in direct contact with the adsorbate solution. Specially designed liquid cells matched for different incidence angles were used to carry out measurements in a range of organic solvents with different refractive indices as the ambient medium. The observed shifts in the ellipsometric phase angles Δ upon monolayer formation were found to depend very sensitively on the incidence angle and the refractive indices of the adsorbate film and the ambient solvent, from which a rather simple method for determining the refractive index of the adsorbate film, based on a variation of the ambient refractive index, was derived. Time-resolved *in situ* measurements of SAM formation in different solvents and onto different substrates yielded accurate kinetic information on the monolayer growth process and revealed hitherto unknown strong solvent effects on the growth rate.

Key Words: in situ **ellipsometry; self-assembled monolayers; refractive index; monolayer growth.**

INTRODUCTION

The adsorption and structural organization of long-chain hydrocarbon compounds onto solid surfaces from dilute solutions under formation of self-assembled monolayers are a widespread phenomenon, which has attracted considerable interest over the past decade (1). A wide variety of surface analytical methods has been applied to study the formation and properties of such films. However, only a few methods allow a direct investigation of film formation at the substrate–solution interface. Correspondingly, few *in situ* studies of these systems have been reported to date, using atomic force microscopy (2, 3), internal reflection spectroscopy (4, 5), or a quartz crystal microbalance (6, 7).

Ellipsometry has proved in the past to be a versatile tool for the investigation of thin films deposited on optically flat substrates (8, 9). One advantage of ellipsometry over many other surface analytical methods is the possibility to perform measurements in different ambient media such as vacuum, normal atmosphere, or liquids. This feature together with the high time resolution and sensitivity of the measurements allows a direct monitoring of gas-phase depositions as well as *in situ* studies of adsorption processes from solution. The vast majority of *in situ* ellipsometric investigations reported in the literature using liquid ambient media concern the physisorption of biomolecules (10–21), polymers (22–25), or cationic surfactants (26–28) onto solid surfaces from dilute, mostly aqueous solutions. In these studies, the adsorbed amount Γ (g m^{-2}), which was taken as an indicator for the surface concentration of adsorbed species, was calculated from the measured film refractive index, the film thickness, and the concentration dependence of the refractive index determined from solution measurements. For ultrathin films such as self-assembled monolayers with a typical thickness of 10–30 Å, this method cannot be applied because film thickness and refractive index cannot be measured simultaneously. Additionally, the extrapolation of solution-phase data to monolayer film properties is not justified in these strongly chemisorbed systems (1).

We report here a procedure which allows a straightforward determination of the film refractive indices of self-assembled monolayers through measurements of the ellipsometric angles in different solvents at different angles of incidence. Furthermore, we present *in situ* ellipsometric measurements of the formation of octadecylsiloxane monolayers on native silicon in different solvents at different concentrations of the adsorbate solutions and show that this method can also be used to monitor subsequent surface modifications and multilayer formation of these films.

MATERIALS AND METHODS

Compounds, Solvents, and Substrates

The following compounds and solvents were commercially available and were used as received: octadecyltrichlorosilane (OTS) (Aldrich, 95%), butyltrichlorosilane (BTS) (Aldrich, 99%), perfluorohexane (3M, p.a.), *n*-hexane (Aldrich, 95+%),

[1] To whom correspondence should be addressed.

0021-9797/99 $30.00

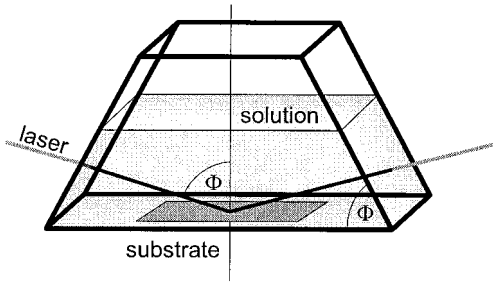

FIG. 1. Schematic design of a liquid cell for *in situ* ellipsometric investigations of the substrate–solution interface. Φ denotes the light incidence angle and the tilt angle of the cell windows with respect to the substrate surface.

cyclohexane (Merck, 99.5+%), tetrachloromethane (Fluka, HPLC grade), toluene (Aldrich, 99.8%), chlorobenzene (Merck, puriss), tribromomethane (Merck, 98%), acetone (Aldrich, 99.9%), and ethanol (Austria Hefe AG, 99.8%). Undecyltrichlorosilane (UTS) and 16-hydroxyhexadecanethiol (HHDT) were synthesized as described previously (29, 30).

Gold-coated glass slides (25×15 mm^2) with preferential (111) orientation, which had been prepared by sputter deposition of approximately 200 nm of gold onto glass slides coated with a thin chromium adhesive layer, were obtained from Pharmacia (Uppsala, Sweden) and were cleaned by ultrasonic treatment in toluene, rinsing with acetone and ethanol and blow-drying in high-purity nitrogen, followed by a 15-min exposure to a UV/ozone atmosphere in a commercial cleaning chamber (Boekel Industries, Model UVClean) equipped with a low-pressure mercury quartz lamp. P-doped, (100)-oriented, single-sided polished silicon wafers (Wacker Chemitronic, test grade, 14–30 Ω cm resistivity, 0.5-mm thickness) were cut into pieces of appropriate size (25×15 mm^2) and were cleaned in the same way as the gold slides. This treatment yields a hydrophilic, contamination-free surface with a native oxide layer of 12- to 14-Å thickness, as routinely checked by ellipsometry.

Ellipsometric Measurements

The ellipsometric measurements were carried out on a Plasmos SD 2300 ellipsometer with a rotating analyzer and a He–Ne laser ($\lambda = 632.8$ nm) as the light source. Film thicknesses and/or refractive indices were calculated from the measured ellipsometric angles (relative phase shift Δ and amplitude ratio Ψ between the s- and p-polarized components of the probing laser) using the commercial instrument software based on the McCrackin algorithm (9). The mechanical suspension of light source and analyzer allowed a continuous change of the angle of incidence between 35° and 73° with respect to the sample surface normal. For *in situ* ellipsometric measurements special liquid cells for incidence angles of 65, 68, and 70° were constructed. The schematic design of such a cell is shown in Fig. 1. The entrance and exit windows have to be inclined under the angle of incidence Φ with respect to the base of the cell to ensure that the incident and reflected laser beams pass through the windows at normal incidence. In this case, the reflection of light at the surface of the cell windows is independent of its direction of polarization and thus the polarization of the probing laser beam is not altered by transmission through the cell windows (9). The liquid cells used for this study were made of microscope glass slides (Menzel Gläser, $76 \times 26 \times 1$ mm^3), which were cut into appropriate size, glued together with epoxy resin, and finally cured for 30 min at 100°C. To avoid any disturbances by solvent evaporation, the cells were closed with a glass lid during the experiments. Possible artifacts caused by cell construction errors were checked by comparison of measurements performed outside and inside the cells under atmospheric conditions. The corresponding differences of the ellipsometric angles Ψ and Δ were never larger than 0.01° for Ψ and 0.1° for Δ, which results in an error less than 1 Å in film thickness for the samples investigated in this study. To perform ellipsometric experiments in a liquid ambient medium, the precleaned substrates were clamped to the bottom of the cell and were aligned in the empty cell under open atmosphere.

Ex Situ Measurements

Ex situ experiments were performed at an incidence angle Φ of 68° on both gold and silicon substrates. On gold, the substrate's optical constants (refractive index n and absorption coefficient k) were first determined using an isotropic model of two semiinfinite phases (air/substrate). Values of $n = 0.165 \pm 0.005$ and $k = 3.57 \pm 0.01$ were reproducibly obtained. The thickness d of an adsorbate film of the film-covered substrates was then measured using an isotropic three-phase model (air/adsorbate/substrate) with the previously determined optical parameters n and k for the gold substrate and assumed values of $n = 1.50$ and $k = 0$ for the adsorbate, the latter representing typical values for nonabsorbing, solid-state organic materials (31). On silicon, an isotropic three-phase model (Si/SiO_2/air) was used for the substrate and a four-phase model (Si/SiO_2/adsorbate/air) for the sample. A measurement of the clean reference Si/SiO_2 yielded the thickness of the native oxide layer using literature values for the optical constants of Si ($n = 3.865$, $k = 0.020$ (32)) and SiO_2 ($n = 1.465$, $k = 0$ (32)). Subsequent measurement of the film-covered substrate and substitution of the substrate parameters together with assumed values for the adsorbate ($n = 1.50$ and $k = 0$) into a four-phase (Si/SiO_2/adsorbate/air) algorithm allowed a calculation of the adsorbate layer thickness. For refractive index determinations of adsorbed films, a silicon substrate was mounted and aligned in the liquid cell under air. Then the cell was filled with solvent and the ellipsometric angles Ψ and Δ were determined. These measurements were carried out for three angles of incidence (65, 68, and 70°) with each of the following solvents: perfluorohexane, *n*-hexane, cyclohexane,

tetrachloromethane, toluene, chlorobenzene, and tribromomethane. Subsequently, the silicon substrate was removed from the cell and a self-assembled monolayer of either butylsiloxane (BS), undecylsiloxane (UDS), or octadecylsiloxane (ODS) was adsorbed, as described in detail elsewhere (29). The monolayer thickness was determined under air, after which the substrate was remounted in the liquid cell and the ellipsometric angles Ψ and Δ were measured again at 65, 68, and 70° incidence in each of the above listed solvents. The experimental error margins were determined from 10 individual measurements at different locations of each sample.

In Situ Measurements

In situ measurements of ODS monolayer formation on silicon substrates were carried out in *n*-hexane at 68° incidence and in perfluorohexane at 70° incidence. The substrate was mounted and aligned in the liquid cell as described above, and the cell was subsequently filled with solvent and closed. After stabilization of the system, start values of the angles Ψ and Δ were measured. The solvent was rapidly exchanged with the adsorbate solution (OTS in *n*-hexane or perfluorohexane) and the ellipsometric angles Ψ and Δ were measured as a function of time. After completion of the adsorption process (Ψ and Δ remain constant within experimental error), the cell was emptied and the sample was dismounted, rinsed with toluene, acetone, and ethanol, and blow-dried in a stream of nitrogen. Finally, the thickness of the ODS monolayer was measured by *ex situ* ellipsometry under air to verify completion of the monolayer formation. A similar experimental procedure was used to follow the formation of an ω-hydroxyalkanethiol monolayer on a gold substrate and its subsequent coupling to an ODS overlayer. A cleaned gold substrate was mounted and aligned under air in the 68° liquid cell. The cell was filled with 5 mL of *n*-hexane and the start values of the ellipsometric angles Ψ and Δ were measured. Immediately afterward, a certain amount of HHDT, corresponding to a concentration of 5×10^{-6} mol/L, was injected into the cell and Ψ and Δ were measured as a function of time. After completion of monolayer formation, a certain amount of OTS, corresponding to a concentration of 10^{-4} mol/L, was added to the same solution and the formation of an ODS overlayer was monitored by the changes of Ψ and Δ with time.

RESULTS AND DISCUSSION

Refractive Index Determinations of Monolayer Films

Figure 2 shows the calculated Brewster angle $\Phi_B = \tan^{-1}(n_{sub}/n_{amb})$ of a silicon substrate ($n_{sub} = 3.865$) as a function of the refractive index n_{amb} for different ambient solvents ranging from perfluorohexane ($n_{amb} = 1.252$) to tribromomethane ($n_{amb} = 1.596$). Within this range of solvents, an essentially linear decrease of Φ_B with increasing n_{amb} is shown in Fig. 2. Strictly speaking, the Brewster angle is defined only for nonabsorbing

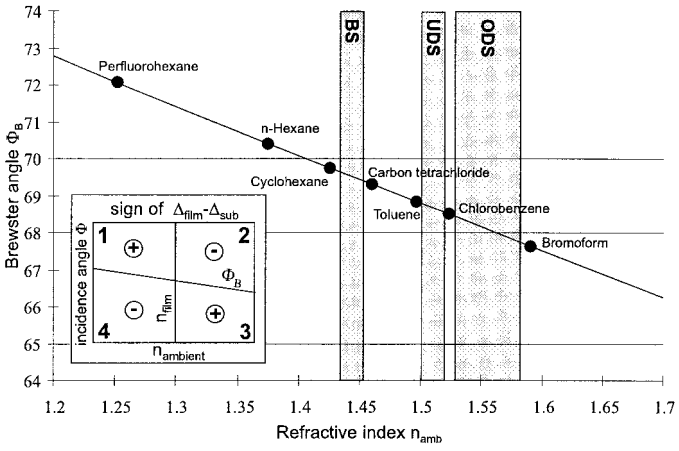

FIG. 2. Brewster angle $\Phi_B = \tan^{-1}(n_{sub}/n_{amb})$ of a silicon substrate ($n_{sub} = 3.865$) immersed in different ambient solvents as a function of the solvent refractive index n_{amb}. The shaded areas represent the determined margins for the refractive indices of monolayer films of butylsiloxane (BS), undecylsiloxane (UDS), and octadecylsiloxane (ODS). The insert illustrates the sign of the difference between the ellipsometric angles Δ of a film-covered silicon substrate Δ_{film} and a clean silicon substrate Δ_{sub} as a function of the light incidence angle Φ and the ambient refractive index n_{amb}. The Brewster angle Φ_B as a function of n_{amb} and the film refractive index n_{film} are marked by solid lines.

substrates as the particular incidence angle, where the propagation vectors of the radiation reflected off the substrate surface and the radiation refracted into the substrate are normal to each other. p-Polarized radiation (electric field vector parallel to the plane of incidence) is therefore totally refracted at Φ_B and the reflectivity is zero. Due to the weak absorptivity of silicon at the probing laser frequency (absorption coefficient $k = 0.02$) and the negligible influence of an ultrathin, transparent adsorbate film on the overall reflectance (33), the optical properties of the film/substrate systems investigated in this study are very similar to those of an ideal, nonabsorbing substrate. Three different incidence angles ($\Phi = 65$, 68, and 70°) in the vicinity of the Brewster angles Φ_B have been used in this study, which are marked by horizontal lines in Fig. 2 and which divide the investigated solvents into two groups, one with $\Phi < \Phi_B$ and one with $\Phi > \Phi_B$. The insert in Fig. 2 shows the results of model calculations based on standard Fresnel equations (8) for the ellipsometric angles Δ_{film} and Δ_{sub} of a monolayer-covered silicon substrate (Δ_{film}) and a clean silicon substrate (Δ_{sub}) for different incidence angles Φ and different ambient media. The sign of $\Delta_{film} - \Delta_{sub}$ falls into one of four sectors, which are separated from each other by the Brewster angle Φ_B and the refractive index n_{film} of the adsorbate film. $\Delta_{film} - \Delta_{sub}$ is positive for incidence angles $\Phi > \Phi_B$ in combination with ambient refractive indices $n_{amb} < n_{film}$ (sector 1) and for $\Phi < \Phi_B$ and $n_{amb} > n_{film}$ (sector 3). A negative sign for $\Delta_{film} - \Delta_{sub}$ is predicted for $\Phi > \Phi_B$ and $n_{amb} > n_{film}$ (sector 2) and $\Phi < \Phi_B$ and $n_{amb} < n_{film}$ (sector 4). Table 1 lists the experimental values $\Delta_{film} - \Delta_{sub}$ for three different alkylsiloxane films (BS, UDS, and ODS) on silicon, measured with

TABLE 1

Ellipsometric Angle Difference $\Delta_{film} - \Delta_{sub}$ between Butylsiloxane (BS), Undecylsiloxane (UDS), and Octadecylsiloxane (ODS) Monolayer Films Adsorbed on Native Silicon Substrates (Δ_{film}) and the Clean Substrates (Δ_{sub}) Measured under Different Incidence Angles in Different Ambient Solvents with Refractive Indices n_{amb} [a]

		$\Phi = 65°$						$\Phi = 68°$		$\Phi = 70°$	
		BS		UDS		ODS		ODS		ODS	
Ambient solvent	n_{amb}	$\Delta_{film} - \Delta_{sub}$	n_{film}(calc)	$\Delta_{film} - \Delta_{sub}$	n_{film}(calc)	$\Delta_{film} - \Delta_{sub}$	n_{film}(calc)	$\Delta_{film} - \Delta_{sub}$	n_{film}(calc)	$\Delta_{film} - \Delta_{sub}$	n_{film}(calc)
Perfluorohexane	1.252	−1.191 ± 0.293	1.440 ± 0.006	−3.794 ± 0.440	1.490 ± 0.04	−3.965 ± 0.383	1.512 ± 0.05	−6.514 ± 0.414	1.598 ± 0.03	−10.898 ± 2.225	1.462 ± 0.07
n-Hexane	1.375	−0.489 ± 0.179	1.432 ± 0.002	−2.647 ± 0.216	1.488 ± 0.01	−2.998 ± 0.210	1.507 ± 0.01	−8.055 ± 0.344	1.548 ± 0.01	−22.325 ± 7.546	1.505 ± 0.08
Cyclohexane	1.426	−0.229 ± 0.099	1.455 ± 0.001	−1.678 ± 0.107	1.486 ± 0.003	−2.512 ± 0.051	1.520 ± 0.003	−9.088 ± 0.339	1.564 ± 0.007	22.080 ± 6.480	1.503 ± 0.04
Tetrachloromethane	1.460	0.105 ± 0.064	1.453 ± 0.005	−0.429 ± 0.037	1.474 ± 0.001	−2.347 ± 0.058	1.539 ± 0.002	−8.319 ± 0.379	1.551 ± 0.006	14.649 ± 1.335	1.594 ± 0.01
Toluene	1.496	0.561 ± 0.122	1.457 ± 0.006	−0.020 ± 0.010	1.497 ± 0.001	−1.297 ± 0.052	1.533 ± 0.002	−11.746 ± 1.632	1.570 ± 0.01	2.867 ± 0.525	1.522 ± 0.005
Chlorobenzene	1.524	1.255 ± 0.200	1.449 ± 0.01	0.069 ± 0.009	1.507 ± 0.001	−0.880 ± 0.033	1.547 ± 0.001	−6.012 ± 0.980	1.547 ± 0.004	1.987 ± 0.137	1.548 ± 0.002
Tribromomethane	1.596					(0.125 ± 0.012) [b]	(1.590 ± 0.001) [b]			(−0.313 ± 0.064) [b]	(1.590 ± 0.002) [b]

[a] The refractive indices of the adsorbate films n_{film}(calc) were calculated from the experimental $\Delta_{film} - \Delta_{sub}$ values as described in the text.

[b] See note (34).

different incidence angles in a series of different solvents. At 65° incidence, BS monolayers yield negative signs for $\Delta_{film} - \Delta_{sub}$ in perfluorohexane, *n*-hexane, and cyclohexane and positive signs in CCl_4, toluene, and chlorobenzene. Because $\Phi_B > 65°$ for all these solvents (see Fig. 2), the sign change within this solvent series must be caused by a transition from sector 3 to sector 4 in Fig. 2, i.e., a change from $n_{amb} < n_{film}$ to $n_{amb} > n_{film}$ between cyclohexane and CCl_4. For UDS films, this sign change shifts to higher ambient refractive indices and occurs between toluene and chlorobenzene, indicating an increase of the film refractive index with increasing chain length of the adsorbate. This trend continues for ODS monolayers, which yield positive $\Delta_{film} - \Delta_{sub}$ values only in a highly refracting solvent such as tribromomethane (34). ODS monolayers were also investigated at 68 and 70° incidence. For $\Phi = 68°$, results similar to those for $\Phi = 65°$ were obtained (negative $\Delta_{film} - \Delta_{sub}$ values from perfluorohexane to chlorobenzene) except for tribromomethane, where the Brewster angle is too close to the incidence angle and the error in determining the angle Δ becomes exceedingly large. For $\Phi = 70°$, the sign for $\Delta_{film} - \Delta_{sub}$ changes twice: Perfluorohexane and *n*-hexane give negative values ($\Phi < \Phi_B$ and $n_{amb} < n_{ODS}$, sector 4), cyclohexane, CCl_4, toluene, and chlorobenzene give positive values ($\Phi > \Phi_B$ and $n_{amb} < n_{film}$, sector 1), and tribromomethane results again in a negative sign ($\Phi > \Phi_B$ and $n_{amb} < n_{film}$, sector 2). Similar changes in the sign of $\Delta_{film} - \Delta_{sub}$ are caused by changing the incidence angle for certain film–solvent combinations. This is shown in Table 2 for BS, UDS, and ODS films on silicon in CCl_4 ($n_{amb} = 1.46$). BS films yield positive signs for $\Phi = 65°$ and $\Phi = 68°$ ($\Phi < \Phi_B$ and $n_{amb} > n_{film}$, sector 3) and a negative sign for $\Phi = 70°$ ($\Phi > \Phi_B$ and $n_{amb} < n_{film}$, sector 2). UDS and ODS films, on the other hand, whose refractive indices are both larger than 1.46, result in negative $\Delta_{film} - \Delta_{sub}$ values for 65 and 68° incidence ($\Phi < \Phi_B$ and $n_{amb} < n_{film}$, sector 4) and positive values for 70° incidence ($\Phi > \Phi_B$ and $n_{amb} < n_{film}$, sector 1).

As a result of these measurements summarized in Tables 1 and 2, the following margins for the refractive indices of the investigated adsorbate films can be derived, which are illustrated as shaded areas in Fig. 2: $1.426 < n_{BS} < 1.460$, $1.496 < n_{UDS} < 1.524$, $1.524 < n_{ODS} < 1.596$. These results confirm a well-documented trend from previous studies (29, 35–37) that the packing density and the degree of structural order in these films decrease with decreasing hydrocarbon chain length, accompanied by a decrease in the film refractive index. In principle, the margins for the film refractive indices could be further narrowed by using a larger set of solvents or solvent mixtures with selected refractive indices. A certain limit for the accuracy achieved with this procedure is given, however, by the experimental error of the $\Delta_{film} - \Delta_{sub}$ values. For a certain incidence angle, the relative error increases with decreasing refractive index difference between film and solvent (Table 1) up to the point where $n_{film} = n_{amb}$, in which case the film optically disappears by a perfect match with the ambient re-

TABLE 2
Ellipsometric Angle Difference $\Delta_{film} - \Delta_{sub}$ and Calculated Film Refractive Indices n_{film}(calc) of Different Monolayer Films on Native Silicon Substrates in Tetrachloromethane ($n_{amb} = 1.460$)

	$\Phi = 65°$		$\Phi = 68°$		$\Phi = 70°$	
Adsorbate film	$\Delta_{film} - \Delta_{sub}$	n_{film}(calc)	$\Delta_{film} - \Delta_{sub}$	n_{film}(calc)	$\Delta_{film} - \Delta_{sub}$	n_{film}(calc)
BS	0.105 ± 0.064	1.45 ± 0.005	0.092 ± 0.045	1.46 ± 0.001	−0.666 ± 0.048	1.45 ± 0.001
UDS	−0.429 ± 0.037	1.47 ± 0.001	−4.911 ± 0.114	1.51 ± 0.001	11.218 ± 3.224	1.52 ± 0.02
ODS	−2.347 ± 0.058	1.54 ± 0.002	−8.319 ± 0.379	1.55 ± 0.006	14.649 ± 1.335	1.55 ± 0.01

fractive index. This latter configuration is the basis of a technique reported by Yakovlev and Irene (38) that takes advantage of the increased sensitivity of ellipsometric measurements for the substrate–film interface if the film is made invisible to the probing radiation by intentional refractive index matching of the ambient phase. In a given solvent, the absolute values of $\Delta_{film} - \Delta_{sub}$ increase sharply as the incidence angle Φ approaches the Brewster angle Φ_B, and the relative error has a minimum somewhere close to Φ_B (note that for $\Phi = \Phi_B$, the reflected light is purely s-polarized and the phase angle Δ between the p- and s-polarized components is therefore experimentally undeterminable). Thus, optimizing the experimental conditions for a particular system is a rather tedious procedure influenced by a number of mutually dependent parameters.

In principle, the film refractive index can also be determined from a single measurement of $\Delta_{film} - \Delta_{sub}$ in a particular solvent by an iterative fitting procedure. Both Δ_{film} and Δ_{sub} can be calculated from standard Fresnel equations (8) using a three-phase model (Si/SiO_2/solvent) for a native silicon substrate and a four phase model (Si/SiO_2/adsorbate/solvent) for the film-covered substrate, if the film refractive index n_{film} and the film thickness d_{film} are known. With $n_{film} = 1.50$ as a first estimate for the film refractive index, the film thickness d_{film} can be measured in contact with air ($n_{amb} = 1$) and these values n_{film} and d_{film} can be used to calculate $\Delta_{film} - \Delta_{sub}$ for a particular solvent as the ambient medium. Varying n_{film} and recalculating $\Delta_{film} - \Delta_{sub}$ until the best fit for the experimental $\Delta_{film} - \Delta_{sub}$ value is obtained yield an improved value for n_{film}, which allows the calculation of an improved film thickness d_{film}. With this new set of values (n_{film}, d_{film}), the whole process is repeated until a satisfactory agreement between the experimental and calculated ellipsometric angles $\Delta_{film} - \Delta_{sub}$ is achieved. In practice, one iteration step is usually sufficient because the film thickness d_{film} measured in contact with air is quite insensitive to the precise value of the film refractive index (varying n_{film} between 1.45 and 1.55 changes the film thickness only on the order of 1 Å). These calculated film refractive indices n_{film}(calc) for BS, UDS, and ODS monolayers in different solvents are included in Tables 1 and 2. Except for some systematic deviations in solvents of low refractive index, where a certain error in the experimental $\Delta_{film} - \Delta_{sub}$ values has the largest effect on the calculated film refractive indices, the n_{film}(calc) values for the different monolayer films in Tables 1 and 2 lie well within the experimentally determined margins for the film refractive indices (Fig. 2) and clearly confirm the observed trend that n_{film} increases with the hydrocarbon chain length of the film molecules.

In Situ Studies of Film Formation

Figure 3 shows the calculated ellipsometric angles Ψ and Δ as a function of film thickness for a hypothetical organic film ($n_{film} = 1.5$) adsorbed on gold and native silicon (Si/SiO_2, SiO_2 thickness 12 Å) in contact with *n*-hexane ($n = 1.375$) as the ambient medium. On both substrates, the angle Ψ (amplitude ratio between s-polarized and p-polarized radiation) changes

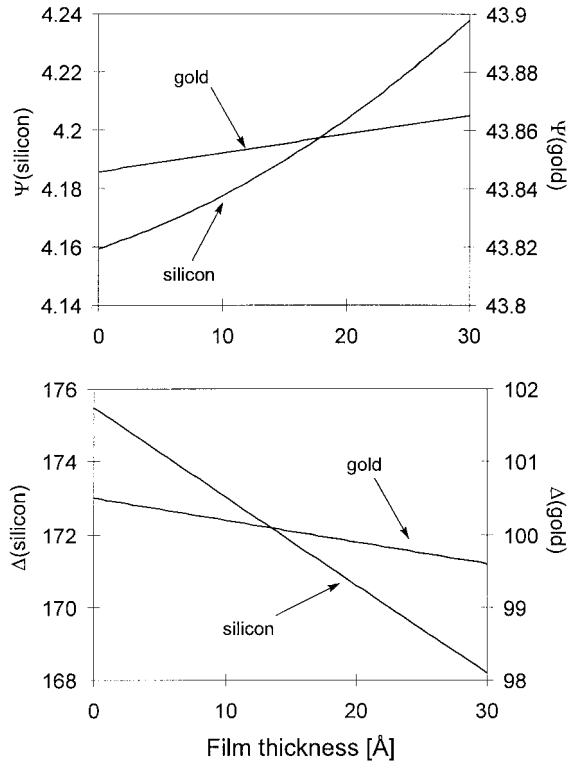

FIG. 3. Calculated ellipsometric angles Ψ and Δ for 68° incidence of a hypothetical adsorbate film ($n_{film} = 1.50$) on a gold and a native silicon substrate (Si/SiO_2) immersed in *n*-hexane as a function of film thickness.

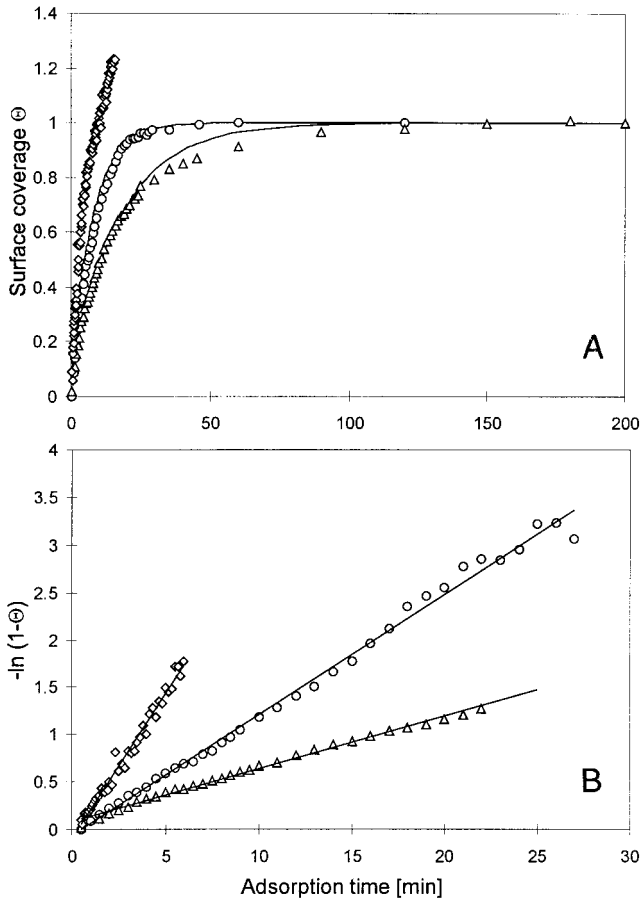

FIG. 4. Surface coverage Θ (A) and $-\ln(1-\Theta)$ (B) as a function of time derived from *in situ* ellipsometric measurements of the adsorption of octadecyltrichlorosilane (OTS) on native silicon substrates from dilute solutions in perfluorohexane for different precursor concentrations c_{OTS}: 5×10^{-5} mol/L (diamonds), 1×10^{-5} mol/L (circles), 5×10^{-6} mol/L (triangles).

very little with thickness for ultrathin films ($0 < d < 30$ Å), whereas the angle Δ (phase shift between s-polarized and p-polarized radiation) is an essentially linear function of d within the considered thickness range. Assuming that the film refractive index does not change significantly in the course of film growth, the Δ values are proportional to the film thickness, and the surface coverage Θ for a monolayer growth process can be obtained as $\Theta = (\Delta_t - \Delta_0)/(\Delta_\infty - \Delta_0)$, where Δ_0, Δ_t, and Δ_∞ are the measured Δ values for the clean substrate, for the adsorbate-covered substrate after an adsorption time t, and for the complete monolayer film. In Figs. 4 and 5, the results of such *in situ* experiments are shown, monitoring the formation of an ODS monolayer film on silicon from dilute solutions of OTS in perfluorohexane (Fig. 4) and in *n*-hexane (Fig. 5) for different OTS concentrations. Except for the highest concentration in perfluorohexane ($c_{OTS} = 5 \times 10^{-5}$ mol/L), the Δ_t values approach a final, constant value Δ_∞, which corresponds to a complete ODS monolayer with a thickness of 26 ± 0.5 Å, as routinely checked after each *in situ* experiment in a control measurement under air. The deviations from this monolayer growth process observed at higher precursor concentrations in perfluorohexane must be ascribed to multilayer deposition of siloxane polymers from solution, because film thicknesses of more than 100 Å were measured for these samples after film deposition. In all other cases, the surface coverages as a function of time calculated from the measured Δ values can be fitted in accordance with previous studies (39) by a simple Langmuirian adsorption model $\Theta = 1 - e^{-ktc}$ based on irreversible adsorption, where k is the adsorption rate constant and c is the precursor concentration in solution. From the logarithmic plots shown in Figs. 4B and 5B, a rate constant of $k = 198 \pm 14$ L mol^{-1} s^{-1} in perfluorohexane and $k = 4.91 \pm 0.20$ L mol^{-1} s^{-1} in *n*-hexane can be derived. The large difference observed between two supposedly inert solvents points to a specific stabilization of the precursor molecules in a pure hydrocarbon solvent such as *n*-hexane, which slows down the adsorption process by more than a factor of 50 in comparison to perfluorohexane. A detailed study of this

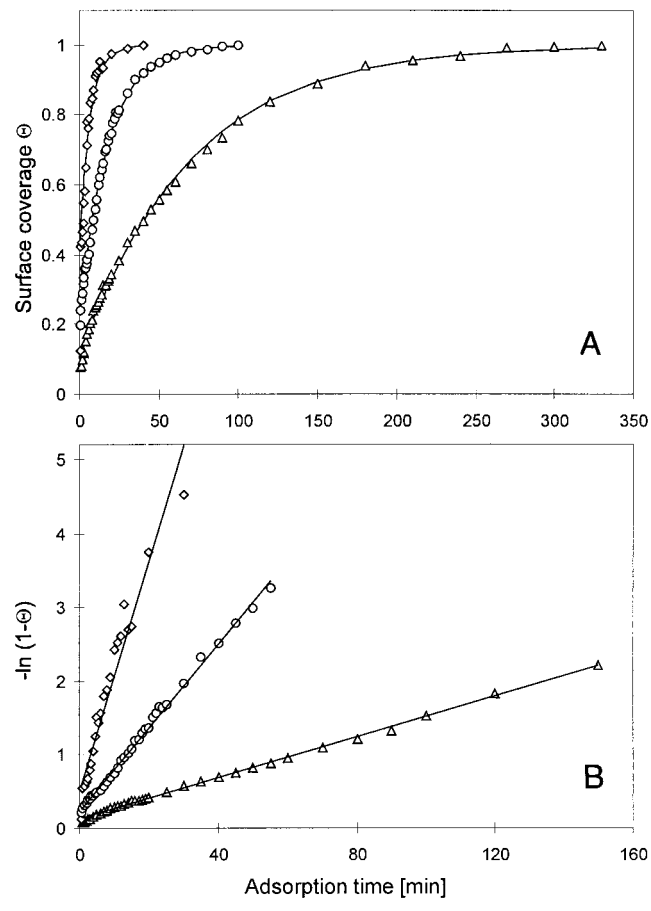

FIG. 5. Surface coverage Θ (A) and $-\ln(1-\Theta)$ (B) as a function of time derived from *in situ* ellipsometric measurements of the adsorption of octadecylsiloxane (ODS) on native silicon substrates from dilute solutions in *n*-hexane for different precursor concentrations c_{OTS}: 5×10^{-4} mol/L (diamonds), 2×10^{-4} mol/L (circles), 5×10^{-5} mol/L (triangles).

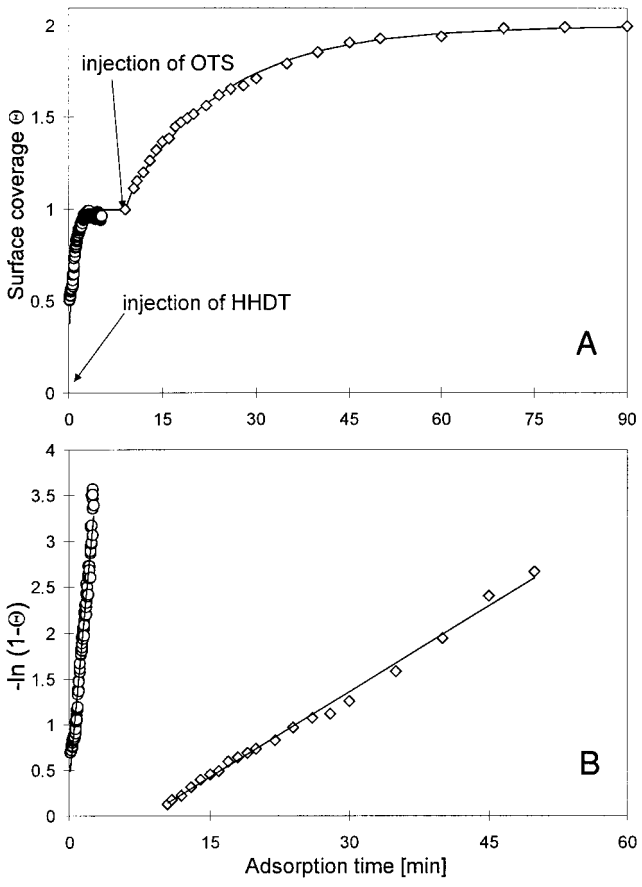

FIG. 6. Surface coverage Θ (A) and $-\ln(1-\Theta)$ (B) as a function of time derived from *in situ* ellipsometric measurements of a two-step adsorption process on a gold substrate. The first step involves the monolayer formation of 16-hydroxyhexadecanethiol (HHDT) from a dilute solution in *n*-hexane. In the second step, an overlayer of octadecylsiloxane is adsorbed on top of the HHDT primer layer.

hitherto unnoticed role of the solvent in the formation of such monolayer films will be published shortly.

As a final example for the potential of *in situ* ellipsometry, a two-step adsorption process on a gold substrate was investigated. In the first step, 16-hydroxyhexadecanethiol (HHDT) is adsorbed on a gold surface from a dilute solution of HHDT ($c = 5 \times 10^{-6}$ mol/L) in *n*-hexane, which results in a monolayer film of thiolate molecules anchored by Au–S bonds to the substrate surface and terminated by surface OH groups (40). An artificial, hydroxylated substrate is therefore created in the first step, onto which a monolayer of ODS can be adsorbed subsequently by injection of the precursor compound OTS into the adsorbate solution. In analogy to the above described experiments on silicon substrates, the ellipsometric angles Δ were monitored and were transformed into surface coverages as a function of time (Fig. 6). Both adsorption steps obey Langmuir adsorption kinetics, whereby the first step (HHDT monolayer formation) proceeds with a substantially higher rate constant ($k \sim 386$ L mol^{-1} s^{-1}) than the second step (ODS monolayer formation), for which a rate constant $k \sim 10.4$ L mol^{-1} s^{-1} similar to the same process on a native silicon surface ($k \sim 5$ L mol^{-1} s^{-1}) is found.

CONCLUSIONS

Ellipsometry is a straightforward and well-established method for investigating adsorption processes at the solid–gas and the solid–liquid interface, although the vast majority of the hitherto reported studies with a liquid ambient medium have been restricted to aqueous adsorbate solutions. The present study extends this latter type of application to a variety of nonaqueous ambient phases. Self-assembled monolayers of long-chain hydrocarbon compounds on native silicon and gold substrates served as well-defined model systems for evaluating the potential and limitations of this method under different liquid environments. With a set of organic solvents with different refractive indices as ambient phases and monolayer films of different alkylsiloxanes on silicon as samples, it was shown that the experimental accuracy of ellipsometric measurements under these conditions depends on a complex interplay of several parameters such as the light incidence angle and the optical properties of solvent and adsorbate. The very sensitive response of the ellipsometric angles to changes in the refractive index of the ambient medium allowed a fairly accurate determination of the refractive indices of the adsorbed monolayer films, which contain important information on the structural properties of these monolayers. Additionally, we have shown that under optimized experimental conditions the formation of such monolayers can be monitored *in situ* from dilute solutions of the corresponding precursor compounds in different organic solvents, yielding accurate kinetic data on the adsorption process with a simple experimental setup and a high time resolution on the order of 1 s, which surpasses most other analytical *in situ* methods for studying adsorption processes in the monolayer and submonolayer regime at the solid–liquid interface.

ACKNOWLEDGMENTS

This work was supported by the Fonds zur Förderung der Wissenschaftlichen Forschung (Project No. P 9749) and the Hochschuljubiläumsstiftung der Stadt Wien.

REFERENCES

1. Ulman, A., *Chem. Rev.* **96,** 1533 (1996).
2. Vallant, T., Brunner, H., Mayer, U., Hoffmann, H., Resch, R., Grasserbauer, M., and Friedbacher, G., *Appl. Surf. Sci.* **140,** 168 (1999).
3. Woodward, J., and Schwartz, D., *J. Am. Chem. Soc.* **118,** 7861 (1996).
4. Cheng, S., Scherson, D., and Sukenik, C., *J. Am. Chem. Soc.* **114,** 5436 (1992).
5. Cheng, S., Scherson, D., and Sukenik, C., *Langmuir* **11,** 1190 (1995).
6. Schneider, T., and Buttry, D., *J. Am. Chem. Soc.* **115,** 12391 (1993).
7. Tang, X., Schneider, T., and Buttry, D., *Langmuir* **10,** 2235 (1994).
8. Azzam, R., and Bashara, N., "Ellipsometry and Polarized Light." North-Holland, Amsterdam, 1989.

9. McCrackin, F., Passaglia, E., Stromberg, R., and Steinberg, H., *J. Res. Natl. Bur. Stand., Sect. A* **67,** 363 (1963).
10. De Feijter, J., Benjamins, J., and Veer, F., *Biopolymers* **17,** 1759 (1978).
11. Cuypers, P., Corsel, J., Janssen, M., Kop, J., Hermens, W., and Hemker, C., *J. Biol. Chem.* **258,** 2426 (1983).
12. Corsel, J., Willems, G., Kop, J., Cuypers, P., and Hermens, W., *J. Colloid Interface Sci.* **111,** 544 (1986).
13. Lakamraju, M., McGuire, J., and Daeschel, M., *J. Colloid Interface Sci.* **178,** 495 (1996).
14. Wahlgren, M., Arnebrant, T., and Lundström, I., *J. Colloid Interface Sci.* **175,** 506 (1995).
15. Elofsson, U., Paulsson, M., and Arnebrant, T., *Langmuir* **13,** 1695 (1997).
16. Wannerberger, K., Welin-Klintström, S., and Arnebrant, T., *Langmuir* **13,** 784 (1997).
17. Sellergren, B., Swietlow, A., Arnebrant, T., and Unger, K., *Anal. Chem.* **68,** 402 (1996).
18. Wahlgren, M., and Arnebrant, T., *Langmuir* **13,** 8 (1997).
19. Elofsson, U., Paulsson, M., Sellers, P., and Arnebrant, T., *J. Colloid Interface Sci.* **183,** 408 (1996).
20. Mårtensson, J., Arwin, H., Lundström, I., and Ericson, T., *J. Colloid Interface Sci.* **155,** 30 (1993).
21. Razumas, V., Nylander, T., and Arnebrant, T., *J. Colloid Interface Sci.* **164,** 181 (1994).
22. Siqueira, D., Breiner, U., Stadler, R., and Stamm, M., *Langmuir* **11,** 1680 (1995).
23. Siqueira, D., Pitsikalis, M., Hadjichristidis, N., and Stamm, M., *Langmuir* **12,** 1631 (1996).
24. Tiberg, F., Malmsten, M., Linse, P., and Lindman, B., *Langmuir* **7,** 2723 (1991).
25. Poncet, C., Tiberg, F., and Audebert, R., *Langmuir* **14,** 1697 (1998).
26. Tiberg, F., and Landgren, M., *Langmuir* **9,** 927 (1993).
27. Tiberg, F., Jönsson, B., Tang, J., and Lindman, B., *Langmuir* **10,** 2294 (1994).
28. Tiberg, F., Jönsson, B., and Lindman, B., *Langmuir* **10,** 3714 (1994).
29. Hoffmann, H., Mayer, U., and Krischanitz, A., *Langmuir* **11,** 1304 (1995).
30. Brunner, H., Vallant, T., Mayer, U., and Hoffmann, H., *Surf. Sci.* **368,** 279 (1996).
31. Parikh, A. N., Allara, D. L., Azouz, I. B., and Rondelez, F., *J. Phys. Chem.* **98,** 7575 (1994).
32. Palik, E., "Handbook of Optical Constants of Solids." Academic Press: New York, 1985.
33. Banga, R., and Yarwood, J., *Langmuir* **11,** 618 (1995).
34. Due to several experimental problems associated with the use of tribromomethane as a solvent (silicon substrates tend to float in such a high-density liquid and the epoxy glue of the cell windows is slowly dissolved), the data obtained from tribromomethane solutions must be taken with caution and may contain some systematic errors.
35. Tillman, N., Ulman, A., Schildkraut, J. S., and Penner, T., *J. Am. Chem. Soc.* **110,** 6136 (1988).
36. Ohtake, T., Mino, N., and Ogawa, K., *Langmuir* **8,** 2081 (1992).
37. Brzoska, J., Azouz, I. B., and Rondelez, F., *Langmuir* **10,** 4667 (1994).
38. Yakovlev, V. A., and Irene, E. A., *J. Electrochem. Soc.* **139,** 1450 (1992).
39. Cheng, S. S., Scherson, O. A., and Sukenik, C. N., *J. Am. Chem. Soc.* **114,** 5436 (1992).
40. Nuzzo, R., Dubois, L., and Allara, D., *J. Am. Chem. Soc.* **112,** 558 (1990).